Annals of Physics 412 (2020) 168011

Contents lists available at ScienceDirect

Annals of Physics

journal homepage: www.elsevier.com/locate/aop

Cuprates and center vortices: A QCD confinement mechanism in a high-T_c context

Jeff Greensite, Kazue Matsuyama *

Physics and Astronomy Department, San Francisco State University, 1600 Holloway Ave, San Francisco, CA 94132, USA

ARTICLE INFO

Article history:
Received 2 December 2018
Accepted 24 October 2019
Available online 13 November 2019

Keywords:
Superconductivity
Phase transitions
Confinement mechanisms
Vortices

ABSTRACT

It is suggested that the center vortex confinement mechanism, familiar in hadronic physics, may have some relevance to high-T_c phenomena. We focus specifically on the transition from the superconducting phase to the pseudogap phase. There is evidence of a vortex liquid in the latter phase, in which the pairing responsible for superconductivity still exists, but superconductivity itself does not. An analogy, drawn from particle physics, may be the Higgs to confinement phase transition in an SU(N) gauge theory, where the confined phase is a vortex liquid, and the Higgs phase is a phase of a broken global Z_N symmetry. We illustrate this idea with numerical simulations of a spatially asymmetric U(1) gauge-Higgs model, with lattice artifact monopoles suppressed. We show the existence of a Higgs (superconductor) to confinement (vortex liquid) phase, explicitly identifying vortices in lattice configurations generated in the confined phase, and showing that they produce an area-law falloff in planar Wilson loops, which may be measurable experimentally. The superconducting phase is a phase of broken global Z_2 symmetry.

1. Introduction

In a series of articles that appeared over a decade ago, Ong et al. [1–3] presented evidence that the pseudogap phase in the cuprates behaves in some ways as a vortex liquid; more recently the

* Corresponding author.
E-mail addresses: greensit@sfsu.edu (J. Greensite), kazuem@sfsu.edu (K. Matsuyama).

https://doi.org/10.1016/j.aop.2019.168011
0003-4916/

idea has been discussed by Anderson [4,5]. Since the evidence presented by Ong et al. also suggests that the pairing responsible for superconductivity persists in the pseudogap region, the question is why superconductivity is absent in this region. The answer given in the cited references (see also [6]) is that superconductivity is a "phase locked" region, where this expression refers to the phase of the order parameter, while the pseudogap region is characterized by spatial disorder in the phase of the order parameter, which is due to the existence of a disordered vortex liquid. Of course a gauge choice, e.g. London gauge, is implicit in this picture, since the phase of the order parameter is a gauge-variant quantity. We will argue here, in the context of an effective U(1) gauge-Higgs theory with a no-monopole constraint, that the vortex liquid and superconductor phases can be distinguished by the unbroken or spontaneously broken realization of a global Z_2 symmetry, and in the process we will make contact with one of the proposed mechanisms of quark confinement, known as the center vortex mechanism, in non-abelian gauge theories.

In Section 2 we introduce a spatially asymmetric lattice version of the 3D Ginzburg–Landau model with a no-monopole constraint, and discuss its symmetries. It is not intended to be a realistic model of high temperature superconductors, but rather to illustrate certain features which we believe are relevant to the superconductor to pseudogap transition in cuprate materials.[1] In Section 3 we briefly review the center vortex confinement mechanism in SU(N) gauge theories, and the importance of global center symmetry in such theories. The results of lattice Monte Carlo simulations of the modified Ginzburg–Landau model are presented in Section 4. Section 5 explores possible connections to spin glasses and the concept of custodial symmetry breaking, and in Section 6 we outline how one might derive and study, with our suggested gauge field observables, a more realistic model of the cuprates. Section 7 contains concluding remarks.

2. The model

We begin with a lattice version of the classical Ginzburg–Landau action (i.e. no time derivatives), which is also known as the $D = 3$ dimensional abelian Higgs model, with a double charged Higgs field

$$\begin{aligned} S_{GL} = & -\beta \sum_x \sum_{\mu=1}^{2} \sum_{\nu=\mu+1}^{3} \cos(\theta_{\mu\nu}(x)) \\ & - \sum_x \sum_{\mu=1}^{3} \mathrm{Re}[\phi^*(x) e^{2i\theta_\mu(x)} \phi(x+\hat{\mu})] \\ & + \sum_x \left[3\phi^*(x)\phi(x) + \lambda(\phi^*(x)\phi(x) - \gamma)^2 \right] , \end{aligned} \tag{1}$$

where

$$\theta_{\mu\nu}(x) = \theta_\mu(x) + \theta_\nu(x+\hat{\mu}) - \theta_\mu(x+\hat{\nu}) - \theta_\nu(x) . \tag{2}$$

We will simplify further by taking the limit $\lambda \to \infty$, and after rescaling the Higgs field and dropping a constant we have[2]

$$\begin{aligned} S' = & -\beta \sum_x \sum_{\mu=1}^{2} \sum_{\nu=\mu+1}^{3} \cos(\theta_{\mu\nu}(x)) \\ & - \gamma \sum_x \sum_{\mu=1}^{3} \mathrm{Re}[\phi^*(x) e^{2i\theta_\mu(x)} \phi(x+\hat{\mu})] , \end{aligned} \tag{3}$$

with the unimodular constraint $\phi^*(x)\phi(x) = 1$.

[1] For a recent, quite different approach to an effective gauge Higgs model for the cuprates, based on a fractionalization of the spin density wave order parameter which results in an emergent non-abelian SU(2) gauge symmetry, see [7].

[2] The couplings β, γ in natural units are $\beta = 1/(e^2 kTa)$, $\gamma = g/(kTa)$, where e is electric charge, g is a dimensionless lattice coupling, T is temperature, and a is the lattice spacing.

The compactness of the U(1) gauge group has one consequence which, in the present context, is very unphysical, namely the existence of magnetic monopoles. These are lattice artifacts which are responsible, in pure compact U(1) gauge theory, for confinement in $D = 3$ spacetime dimensions. In order to suppress these objects entirely we insert a constraint in the integration measure which prevents their appearance. The number of monopoles at a site on the dual lattice, in $D = 3$ dimensions, is determined from the $\theta_\mu(x)$ angular variables by the DeGrand–Toussaint [8] construction. The no-monopole constraint [9] is a Kronecker delta in the lattice measure which ensures that the monopole number is zero at every site of the dual lattice.

In cuprates the pairing phenomenon occurs, by some mechanism, in two dimensional planes, while the electromagnetic field extends, as usual, in three space dimensions. In order to include some remnant of this feature in our model, we simply eliminate the hopping term for the Higgs field in the third spatial dimension

$$S_{MGL} = -\beta \sum_x \sum_{\mu=1}^{2} \sum_{\nu=\mu+1}^{3} \cos(\theta_{\mu\nu}(x)) - \gamma \sum_x \sum_{\mu=1}^{2} \mathrm{Re}[\phi^*(x) e^{2i\theta_\mu(x)} \phi(x+\hat{\mu})] \ , \tag{4}$$

while retaining the unimodular constraint on the Higgs field. This "modified Ginzburg–Landau" action, together with the no-monopole constraint, is the theory we will focus on. It is of course not intended as a realistic effective action for high T_c phenomena. The intention is only to illustrate one particular aspect mentioned in the Introduction, namely, the nature of the transition between a Higgs phase, and a vortex liquid (or "confining") phase, which we think may have some relevance to the superconducting to pseudogap transition in the cuprates.

The action S_{MGL} is invariant under three distinct symmetries:

1. local U(1) gauge symmetry;
2. global Z_2 symmetry;
3. a set of global U(1) symmetries in the Higgs sector, one for each xy plane.

2.1. Gauge symmetry

We need not elaborate on local U(1) symmetry, apart from making one important point. Some textbooks on quantum field theory erroneously describe the Higgs phase of the theory, which is the phase of superconductivity in the condensed matter context, as a phase in which the local gauge symmetry is spontaneously broken. The description is erroneous for the simple reason that a local gauge symmetry cannot break spontaneously, as proven many years ago by Elitzur [10]. In fact, for a Higgs field with a single unit of charge, there is no thermodynamic transition in the $\beta - \gamma$ plane which completely isolates the confined and Higgs regions of the theory. The proof is due to Osterwalder and Seiler [11], and its implications were elucidated by Fradkin and Shenker [12]. One consequence, which applies to the double-charged Higgs case as well, is that neither the magnitude nor the phase of the Higgs field ϕ can be regarded as an order parameter, since

- $\langle \phi \rangle = 0$ at all β, γ in the absence of gauge fixing;
- $\langle \phi \rangle = 1$ at all β, γ in unitary gauge, even in the massless phase;
- in other gauges $\langle \phi \rangle$ may be zero or non-zero at a particular β, γ, depending on the gauge choice [13].

This does not mean that there is no precise distinction between, say, the Higgs and confinement regions. It does mean that a fictitious breaking of the gauge symmetry cannot be used to make that distinction.

2.2. Global Z_2 symmetry

In the case of a double-charged Higgs field, the Higgs phase is distinguished by the spontaneous breaking of a global Z_2 symmetry. This global transformation can be applied to gauge link variables

$$U_\mu(x) = e^{i\theta_\mu(x)} \tag{5}$$

on any given plane orthogonal to one of the coordinate axes.

Consider, e.g., any y, z plane at constant x, e.g. $x = 1$, and make the transformation

$$\begin{aligned} U_1(\boldsymbol{x}) &\to \sigma U_1(\boldsymbol{x}) \ , \quad x = 1, \ \text{all} \ \ y, z \\ \sigma &= \pm 1 \in Z_2 \ . \end{aligned} \tag{6}$$

The action S_{MGL} is invariant under this transformation. It is also invariant under transformations in any other plane:

$$\begin{aligned} U_3(\boldsymbol{x}) &\to \sigma U_3(\boldsymbol{x}) \ , \quad z = 1, \ \text{all} \ \ x, y \\ U_2(\boldsymbol{x}) &\to \sigma U_2(\boldsymbol{x}) \ , \quad y = 1, \ \text{all} \ \ x, z \ . \end{aligned} \tag{7}$$

where indices 1,2,3 correspond to spatial directions x, y, z respectively

A Polyakov line is a Wilson loop along a line running in either of the x, y, z directions, which is closed by lattice periodicity; e.g.

$$P(y, z) = \prod_{x=1}^{N_x} U_1(x, y, z) \ , \tag{8}$$

where N_x is the number of lattice sites in the x direction. Under the Z_2 transformation (6), the Polyakov line transforms by $P(y, z) \to \sigma P(y, z)$. We take the lattice extension in the x direction to be arbitrarily large but fixed, and take limit of large extension in the y, z directions. Since the action is invariant under the global Z_2 symmetry, but the Polyakov line is not, the expectation value $\langle P \rangle$ is, in the limit of large y, z area, a gauge-invariant order parameter for the spontaneous breaking of this symmetry. The Polyakov line expectation value is often applied, in QCD studies, to detect the high-temperature deconfinement phase. But it also serves to detect the breaking of global Z_2 symmetry in the Higgs/superconductor phase, and to rigorously distinguish that phase from other phases of the system, when the scalar field carries two units of electric charge.

2.3. Global $U(1)$ symmetries

The action S_{MGL} is also invariant under transformations of the Higgs field

$$\phi(\boldsymbol{x}) \to e^{i\alpha(z)}\phi(\boldsymbol{x}) \ , \tag{9}$$

which are local in the z-direction, but global in any x–y plane; these can be regarded as a set of independent global U(1) transformations on each x–y plane. A related symmetry in the Higgs sector, sometimes known as "custodial symmetry" (see, e.g., [14,15]) does play a role in non-abelian gauge-Higgs theories when the Higgs field is in the fundamental representation, and may even (despite the Fradkin–Shenker argument [12] based on the Osterwalder–Seiler theorem [11]) serve to distinguish a Higgs from confinement phase in such theories [16]. In the present case this global symmetry in the x–y planes might appear to be irrelevant, owing to the fact (the Mermin–Wagner theorem) that continuous global symmetries cannot break in two dimensions. Nevertheless, we believe that this symmetry does play a role in distinguishing the gapped from ungapped phases. The discussion will be postponed to Section 5.

3. Center symmetry and center vortices

In this section we will take a short excursion into confinement physics in SU(N) non-abelian gauge theories, before returning to the abelian theory described by S_{MGL}. The relevance of center vortices to confinement was first pointed out by 't Hooft [17]; an extensive review of the confinement mechanisms which have been proposed for non-abelian gauge theories is found in Ref. [18,19]. Here we provide only the briefest summary of ideas which are directly relevant to this article.

The center of a group is the set of all elements which commute with all other elements of the group. For an SU(N) group this is the set

$$\{z_n \mathbb{1} = e^{2\pi i n/N}\mathbb{1},\ n = 0, 1, \ldots, N-1\}\ , \tag{10}$$

where $\mathbb{1}$ the $N \times N$ unit matrix, and $Z_N \in$ SU(N) is the subgroup composed of these center elements. The N-ality k of a group representation $R[g]$, $g \in SU(N)$ is defined by the representation of the center subgroup, i.e.

$$R[zg] = z^k R[g] \quad \text{for} \quad z \in Z_N\ . \tag{11}$$

The fundamental representation has N-ality $k = 1$, and the adjoint representation has N-ality $k = 0$. An SU(N) gauge theory with either no matter fields, or with matter fields only in zero N-ality representations, has a global Z_N center symmetry whose unbroken or broken realization corresponds to the presence or absence of confinement. "Confinement" means here that the interaction potential between static test charges in the fundamental and anti-fundamental representations, at large color charge separation R, rises linearly with R as $R \to \infty$.

An example of a global center transformation in an SU(N) lattice gauge theory is a transformation applied to all timelike link variables $U_0(\mathbf{x}, 0)$ at time $t = 0$:

$$U_0(\mathbf{x}, 0) \to z U_0(\mathbf{x}, 0) \quad , \quad z \in Z_N\ . \tag{12}$$

It is easy to check that the action, and any contractible Wilson loop, is invariant under this transformation. On the other hand a Polyakov loop, which is a Wilson loop winding once around the lattice in the periodic time direction, transforms as $P \to zP$. Since the expectation value of P is the exponential of minus the free energy of an isolated charge, it follows that color charges are confined if $\langle P \rangle = 0$ and center symmetry is unbroken, while they are unconfined in the opposite case $\langle P \rangle \neq 0$ and center symmetry is broken.

One of the most striking features of confinement in an SU(N) gauge theory with center symmetry is the fact that the confining force between color charges, at sufficiently large charge separation, is sensitive only to the N-ality of the color charges, rather than the particular group representation of that N-ality. In other words, let $W_r(C)$ represent the expectation value of a Wilson loop around closed contour C, with the gauge field in representation r. Then for large loops

$$W_r(C) \sim e^{-\sigma_k A(C)}\ , \tag{13}$$

where $A(C)$ is the minimal area enclosed by the loop, and k is the N-ality of representation r. The point is that the string tension σ_k depends only on N-ality of r. If we are to attribute confinement to some special class of configurations which dominate the functional integral at large scales, then we must look for configurations which affect loops in different representations, but with the same N-ality, in the same way. The only known configurations which have this property are called "center vortices".

In a time slice in $D = 4$ Euclidean dimensions, a center vortex is a tubelike structure closely analogous to an Abrikosov vortex in superconductivity, in the sense of being a field configuration carrying a quantized amount of (something analogous to) magnetic flux. The action density of such configurations is concentrated in a region of codimension two. This means that a center vortex is point-like in two Euclidean dimensions, line-like in three dimensions, and surface-like in four dimensions (one may imagine a tube sweeping out a surface-like region in time), with the qualifier "like" meaning that in each case the vortex region has a finite thickness. For an Abrikosov vortex

$$\begin{aligned} W(C) &\equiv \exp\left[i\frac{e}{\hbar} \oint_C d\mathbf{x} \cdot A \right] \\ &= -1\ , \end{aligned} \tag{14}$$

where the loop C runs around the vortex, outside the vortex core. The analogous statement in a non-abelian gauge theory is that if one creates a center vortex topologically linked to a Wilson loop in a representation r of N-ality k running around contour C, the loop is transformed by a center element $z \neq 1$, i.e.

$$W_r(C) \to z^k W_r(C) \ . \tag{15}$$

3.1. Confinement

Confinement in the vortex picture works as follows. Let the gauge group be SU(2) for simplicity. Consider a plane of area L^2 which is pierced, at random locations, by N center vortices, and consider a Wilson loop of area A, in a representation of N-ality $k = 1$ lying in that plane. Then the probability that n of those N vortices will lie inside the area A is

$$P_N(n) = \binom{N}{n} \left(\frac{A}{L^2}\right)^n \left(1 - \frac{A}{L^2}\right)^{N-n} \ . \tag{16}$$

Each vortex piercing the Wilson loop contributes a factor of -1, so the vortex contribution to the Wilson loop is

$$W(C) = \sum_{n=0}^{N} (-1)^n P_N(n) = \left(1 - \frac{2A}{L^2}\right)^N \ . \tag{17}$$

Now keeping the vortex density $\rho = N/L^2$ fixed, and taking the $N, L \to \infty$ limit, we arrive at the Wilson loop area law falloff

$$W(C) = \lim_{N\to\infty} \left(1 - \frac{2\rho A}{N}\right)^N = e^{-2\rho A} \ . \tag{18}$$

That is the center vortex confinement mechanism in three lines [20]. It is the simplest such mechanism known. The crucial assumption is that vortex piercings in the plane are random and uncorrelated, and this implies that vortices percolate throughout the spacetime volume.

There is a great deal of numerical evidence in favor of this picture, obtained from lattice Monte Carlo simulations. Most of this numerical work makes use of a technique, known as "center projection", for locating center vortices in lattice configurations. The idea is to map SU(N) lattice configurations into Z_N configurations, which have only vortex excitations. This is accomplished by a gauge transformation into "maximal center gauge", which brings the SU(N) link variables as close as possible, on average, to the Z_N center elements of the group. Maximal center gauge maximizes the quantity

$$R = \sum_{x,\mu} |\mathrm{Tr}[U_\mu(x)]|^2 \ , \tag{19}$$

which is equivalent to Landau gauge fixing of link variables in the adjoint representation. One then maps each link variable to the closest Z_N center element. What is remarkable is that the center projected configurations are qualitatively, and to a large extent quantitatively, similar to the full SU(N) configurations, in terms of confinement, chiral symmetry breaking, and even the mass spectrum. There is also a simple technique for removing center vortices from the SU(N) configurations. When this is done, confinement and chiral symmetry breaking disappear. For older reviews, see [18,19]. For more recent developments, see [21,22].

3.2. The Higgs phase

Confinement is lost, in a non-abelian theory in $D \leq 4$ dimensions, when the global center symmetry of the action is broken spontaneously, either at high temperatures (this is known as the "deconfinement" transition), or via a transition to a Higgs phase. In the latter case, the action

contains one or more Higgs fields ϕ transforming in the adjoint representation of the gauge group. On the lattice, in d Euclidean spacetime dimensions, the Higgs action has the form

$$S_H = -\sum_x \sum_{\mu=0}^{d-1} \mathrm{Re}[\phi^\dagger(x) U^A_\mu(x)] \phi(x+\hat{\mu}) + \sum_x \{ d\phi^\dagger(x)\phi(x) + V[\phi(x)] \} \ , \tag{20}$$

where $V(\phi)$ is the Higgs potential, and the superscript A in U^A_μ means that the link variables are taken to be in the adjoint representation of SU(N). Since U^A is invariant under transformations $U \to zU$, where $z \in Z_N$, the gauge-Higgs action is invariant under the global center symmetry defined above.

The distinction between the confinement and Higgs phases of gauge theories with adjoint Higgs fields is nicely represented by the behavior of the Wilson loop $W(C)$ and its dual in $D = 4$ dimensions, known as the 't Hooft loop $B(C)$ [17], which can be thought of as a center vortex creation operator. In the confinement phase, Wilson loops fall with the area and the expectation value of 't Hooft loops fall with the perimeter of the loop; in the Higgs phase it is the reverse.

Alternatively, on a finite lattice the Polyakov line is defined by (8), only generalized to the non-abelian gauge group and (on the lattice) the SU(N) link variables. Now if we take one of the Euclidean directions (say $\mu = 0$) to be the time direction, the Polyakov line in the time direction is

$$P(\boldsymbol{x}) = \mathrm{Tr} \left[\prod_{t=1}^{N_t} U_0(\boldsymbol{x}, t) \right] \ . \tag{21}$$

This observable is gauge-invariant, but transforms by a center element $z \in Z_N$ under a global center transformation. It is therefore an order parameter for spontaneous symmetry breaking of global center symmetry. If we keep the time extension arbitrarily large but fixed, and take the large volume limit in the remaining space directions, then the Higgs phase is the phase in which $\langle P \rangle \neq 0$. This is because the Polyakov line is related to the free energy F_q of an isolated static color charge by

$$\langle P \rangle = e^{-N_t F_q} \ . \tag{22}$$

It follows that when $\langle P \rangle = 0$ the free energy of an isolated charge is infinite, and quarks are confined. Conversely, when $\langle P \rangle \neq 0$ the free energy is finite, and quarks are unconfined. In this sense, keeping one (time) direction constant, although arbitrarily large, in the limit that the lattice extension in the space directions are taken to infinity, we may say that the Higgs phase is a phase of spontaneously broken center symmetry.

The analogy we pursue in this paper is that the pseudogap phase in the cuprates is, in the same sense, a phase of unbroken Z_2 global symmetry, and corresponds to the confinement phase in an SU(N) gauge theory, which is a phase of unbroken Z_N center symmetry. These phases can each be regarded as a vortex liquid of some kind. Likewise, the superconducting phase in the cuprates, and the Higgs phase in a gauge theory, correspond to the spontaneously broken phase of global Z_2 and Z_N symmetry, respectively.

In the case of SU(N) gauge theories such as QCD, with matter in the fundamental representation of the gauge group, the action breaks global center symmetry explicitly, $\langle P \rangle$ is always non-zero, and Wilson loops fall off asymptotically with a perimeter law. Moreover there is no thermodynamic transition isolating the Higgs from the confinement regions [11,12]. One may ask in what sense these theories are confining, apart from the fact that the asymptotic spectrum consists of massive color singlets. This is, in fact, a surprisingly subtle question. Our view is presented in Ref. [23].

4. Numerical results

4.1. Pure gauge field

We first consider the three dimensional gauge theory with $\gamma = 0$; i.e. no coupling to the scalar field. Our proposed effective theory eliminates monopoles by a constraint. Without this constraint

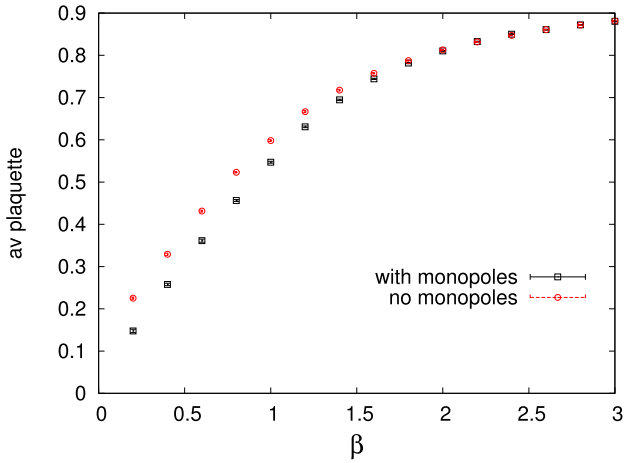

Fig. 1. Average plaquette values in pure compact U(1) lattice gauge theory in D=3 dimensions, with and without the no-monopole constraint.

there is confinement in 2+1 dimensional compact U(1) gauge theory, in the sense of a linearly rising potential between static charges, as we know from the classic work of Polyakov [24]. With the no-monopole constraint this linear confinement property ought to disappear, and the potential between static charges should increase only logarithmically, as in the free continuum theory. This is the first thing to check.

Fig. 1 is a comparison of the average plaquette $\langle \cos\theta_{\mu\nu} \rangle$ vs. β, in compact U(1) theory with and without monopoles. The plaquette averages in the two theories converge as β increases as expected, since the monopole density in the unconstrained theory falls rapidly beyond $\beta = 1$. However, there is a finite monopole density at any β, and even if the difference in average plaquette with and without monopoles is negligible, the unconstrained theory has a linear static potential, while the constrained theory does not. To see this numerically, we note that the potential $V(R)$ between static opposite charges is given by the logarithmic time derivative of rectangular Wilson loops

$$V(R) = -\lim_{T\to\infty} \frac{d}{dT} \log W(R,T) \ . \tag{23}$$

On the lattice we extract $V(R)$ from a best linear fit to the data for $-\log W(R,T)$ vs T, at $T > 10$.

Of course the word "potential" should not be taken too literally in this particular context. $V(R)$ is indeed the potential between static charges in a U(1) theory with two space dimensions and one time dimension, and a linearly rising potential would imply confinement of electric charge. But in three space dimensions it is simply a diagnostic of the behavior of $W(R,T)$ at large R or large T due to thermal fluctuations of the magnetic **B** field. In particular, if $V(R)$ is asymptotically linear at large R, this just means that the Wilson loop falls off exponentially with the area RT enclosed by the loop.

With that caveat, let us compare the potential $V(R)$ in the compact U(1) theory with and without the no-monopole constraint. In a free theory in 2+1 dimensions we expect the potential between static opposite charges to rise logarithmically with charge separation, while in the compact U(1) theory, without any constraint, one expects to see a linear potential. The result of a simulation at $\beta = 2$ is shown in Fig. 2. We find that the potential rises logarithmically in the compact U(1) theory, as in the free theory, when a no-monopole constraint is imposed. The unconstrained compact U(1) theory displays a linearly rising potential, as expected. Note that this drastic difference in the potential is displayed at a coupling $\beta = 2$ where we also see, from Fig. 1, that the difference in average plaquette values in the constrained and unconstrained theories is almost imperceptible.

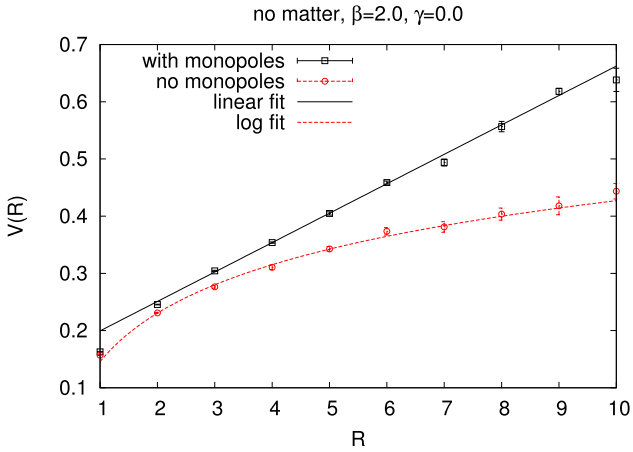

Fig. 2. The potential between static charges of opposite sign in pure compact U(1) gauge theory, D=3 dimensions, at gauge coupling $\beta = 2.0$, with and without the no-monopole constraint. The potential rises linearly in the unconstrained case, but only logarithmically with no monopoles, as in the free (non-compact) gauge theory.

4.2. Modified Ginzburg–Landau

We now couple the scalar field to the gauge field by setting $\gamma > 0$ in (4). The first task is to determine the phase diagram in the space of $\beta - \gamma$ couplings. There is only one symmetry which can be spontaneously broken, namely the global Z_2 symmetry discussed in Section 2.2, and the appropriate order parameter is a Polyakov line running in a direction parallel to the x or y axes. The superconducting region can only be the region where this global Z_2 symmetry is broken, and to check this we look for evidence in the potential, extracted from Wilson loops, that the photon has acquired a mass.

Our numerical simulations are carried out on a 40^3 lattice volume. In the superconducting region we find $\langle P \rangle \neq 0$, while in the normal region we have $\langle P \rangle = 0$ within error bars. The transition points are estimated, on the cubic lattice, by looking for a peak in the Polyakov line susceptibility, either at fixed γ and varying β, or at fixed β while varying γ. Examples of our data for the Polyakov line and the Polyakov line susceptibility vs. β, at fixed $\gamma = 6$, are shown in Figs. 3(a) and 3(b) respectively. The resulting phase diagram is shown in Fig. 4, but since the phase boundary (just drawn as straight lines between the numerically determined transition points) is determined from the breaking of global Z_2 symmetry, the labeling of the different regions (SC, vortex liquid, log potential) must be justified.

We begin at $\gamma = 6$, comparing $V(R)$ calculated from $W(R, T)$ in the x–y plane, as explained above. Fig. 5 displays $V(R)$ calculated just outside the SC region, at $\beta = 1.1$ in a region labeled "vortex liquid", and $V(R)$ just inside the SC region, at $\beta = 1.3$. The potential in the vortex liquid region is fit to the form

$$V(R) = a + b \log(R) + \sigma R \ , \tag{24}$$

and we find from the fit that $\sigma = .00623(8)$, i.e. a "confining" potential, meaning that Wilson loops fall off asymptotically with loop area. In contrast, inside the SC region, we see that $V(R)$ is nearly constant for $R > 3$, consistent with what one would expect from a finite-range interaction mediated by a massive photon. This is evidence of superconductivity in the SC region.

We have labeled the region at small β and large γ, outside the SC domain, as a "vortex liquid", and this characterization must now be justified. Let us consider going to unitary gauge, $\phi(x) = 1$, and taking the $\gamma = \infty$ limit. In this case, the $U_k(x)$ link variables in the x, y directions are forced to be $U_k = \pm 1$, i.e. the variables of a Z_2 gauge theory, at least in the xy planes. The only excitations

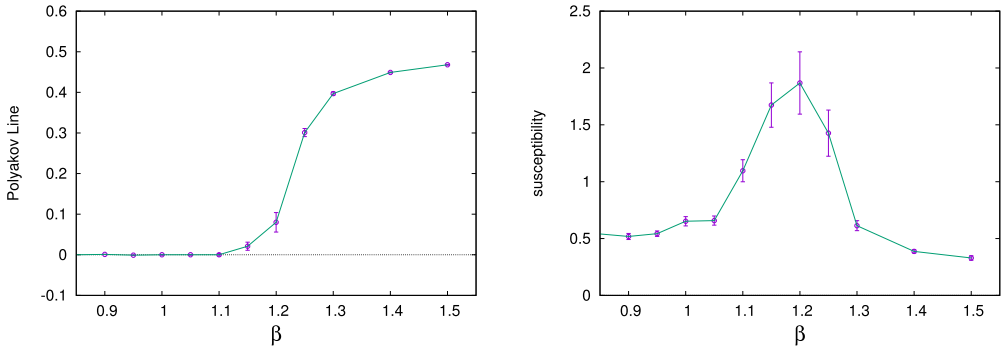

(a) Polyakov line (b) Susceptibility

Fig. 3. (a) Polyakov lines and (b) Polyakov line susceptibilities vs. β at $\gamma = 6$ on a 40^3 lattice volume. All Polyakov lines are 40 lattice units in length, computed in the x and y directions in xy planes.

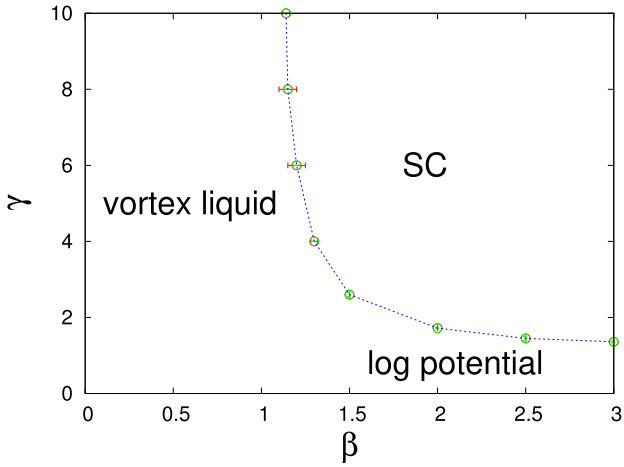

Fig. 4. Phase diagram of the modified Ginzburg–Landau theory in the $\beta - \gamma$ coupling plane. The superconducting phase is also a phase of broken global Z_2 symmetry.

in these planes are at plaquettes where $\cos\theta_{12}(x) = -1$, and these are Z_2 vortex configurations. Consider a Wilson loop

$$W(R,T) = \langle U(R,T) \rangle \ . \tag{25}$$

where $U(R,T)$ is a product of U(1) link variables around a rectangle oriented in one of the x, y planes. Suppose, in some gauge field configuration, there are n plaquettes within this rectangle with $\cos\theta_{12}(x) = -1$. Then

$$U(R,T) = (-1)^n \tag{26}$$

in this $\gamma = \infty$ limit. If there is a finite density of vortices in the plane, and if vortex positions are entirely uncorrelated, then this leads to an area law falloff of $W(R,T)$, and a linear potential for $V(R)$, as explained in Section 3. If there is some finite range correlation among the vortices, then there

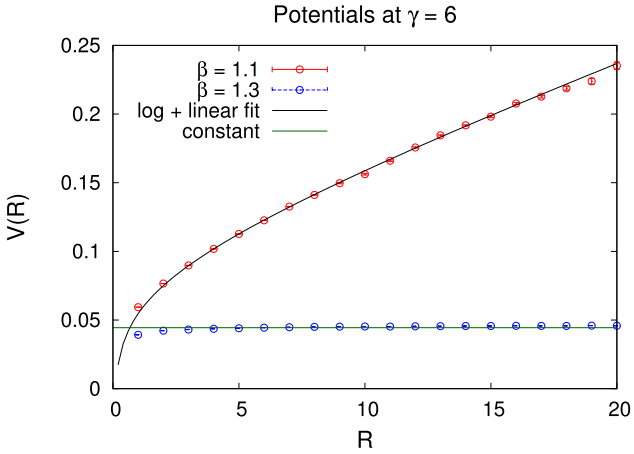

Fig. 5. The potential $V(R)$ at $\gamma = 6$ just outside ($\beta = 1.1$) and just inside ($\beta = 1.3$) the superconducting region.

will be a deviation from the linear potential up to that finite range. A linear potential is therefore the signature that the system in a plane is a disordered gas or liquid of Z_2 vortices.[3]

We can try to locate vortices in xy planes away from the $\gamma = \infty$ limit, with the strategy of (i) performing a gauge transformation which brings link variables in the xy planes as close as possible to ± 1; and (ii) "Z_2 projection" in the xy planes, i.e. projecting link variables in the x, y directions onto the closest element of the Z_2 subgroup of the U(1) gauge group. The gauge transformation should maximize the quantity

$$Q = \sum_x \sum_{i=1}^{2} \cos^2 \theta_i(x) \ , \tag{27}$$

and this is done by performing a sequence of gauge-fixing sweeps of the lattice. In this gauge there is a remnant local Z_2 gauge symmetry. Gauge transformations are made site-by-site, at each site making a transforming which maximizes

$$\sum_{i=1}^{2} \Big[\cos^2 \theta_i(x) + \cos^2 \theta_i(x - \hat{i}) \Big] \ . \tag{28}$$

This procedure converges to a local maximum of Q.[4] The gauge fixing sweeps end when the fractional increase in Q from one sweep to the next falls below 10^{-8}. Z_2 projection consists of the mapping

$$U_i(x) \to Z_i(x) = \text{sign}[\text{Re}(U_i(x))] \quad , \quad i = 1, 2 \ . \tag{29}$$

We define $Z(R, T)$ as the product of projected link variables $Z_i(x)$ around an $R \times T$ rectangle, with the corresponding expectation values

$$W_{proj}(R, T) = \langle Z(R, T) \rangle \ , \tag{30}$$

and we compute the projected potential $V_{proj}(R)$ from the $W_{proj}(R, T)$ by the same procedure used to obtain $V(R)$ from $W(R, T)$. In Fig. 6 we compare $V(R)$ and $V_{proj}(R)$ vs. R, at $\gamma = 6$, $\beta =$

[3] Of course it must be kept in mind that even in the $\gamma = \infty$ limit we are not dealing with a trivial Z_2 gauge theory in two dimensions, since even in this limit the gauge field extends into all three spatial dimensions. For the action S' in (3), the $\gamma = \infty$ theory would be Z_2 gauge theory in three dimensions.

[4] Finding the global maximum is likely to be an NP hard problem.

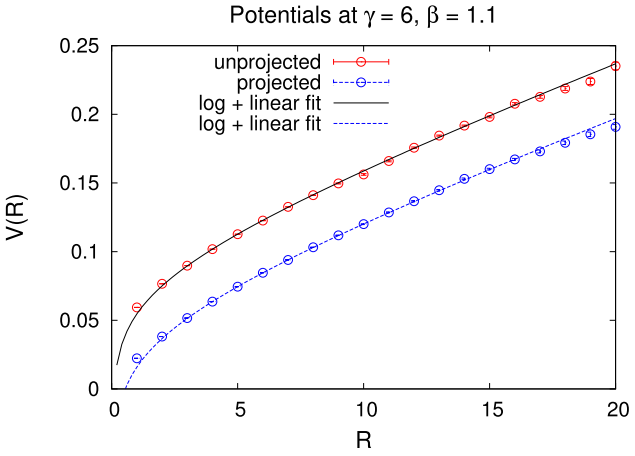

Fig. 6. A comparison of the projected and unprojected potentials, $V(R)$ and $V_{proj}(R)$, at a point in the vortex liquid region.

1.1, and it can be seen that the projected and unprojected potentials are essentially parallel, differing only by a constant R-independent self-energy. Since the vortices alone, in the projected configuration, reproduce the potential in the unprojected lattice, it seems reasonable to attribute the R-dependence of the potential to the effects of vortices, whose positions in the unprojected lattice are located by the excitations in the projected lattice. As a further check we can compute the average value of $\cos\theta_{\mu\nu}(x)$ for plaquettes on the original lattice, at locations where the plaquette on the projected lattice is -1, indicating the presence of a Z_2 vortex. At couplings $\beta = 1.1, \gamma = 6$, these special "vortex plaquettes" have an average value of 0.398, to be compared with the average over all plaquettes, which is $\langle\cos(\theta_{\mu\nu}(x))\rangle = 0.909$. So although the procedure for locating vortices involves fixing to a particular gauge (i.e. maximal Z_2 gauge), we nevertheless find that the locations of vortices on the projected lattice are very strongly correlated with a gauge-invariant observable on the unprojected lattice, i.e. the gauge-invariant field strength.[5]

For these reasons we label the region where a linear potential can be identified, and where the projected and unprojected string tensions agree, as a "vortex liquid". The linear potential disappears in both the projected and unprojected potentials inside the SC region, as seen in Fig. 7 for $\gamma = 6,\ \beta = 1.3$.

Linear confinement cannot persist down to $\gamma = 0$, simply because the theory in that limit is pure U(1) gauge theory, and with the no-monopole constraint there are no topologically stable configurations which could disorder Wilson loops. And at small but finite γ we cannot, in fact, detect any string tension from numerical simulations. Fig. 8 shows our data for $V(R)$ at $\beta = 2.5$ just below ($\gamma = 1.4$) and just inside ($\gamma = 1.55$) the SC phase. Just below the SC phase, at $\beta = 2.5,\ \gamma = 1.4$, the potential fits a logarithm, i.e. it is consistent with Eq. (24) with $\sigma \approx 0$, which is the fit shown in Fig. 8. Inside the SC phase at $\beta = 2.5,\ \gamma = 1.55$ the potential is nearly flat, as expected.

In a region where the potential is logarithmic, i.e. essentially perturbative, we would not expect to explain the potential via purely non-perturbative effects due to vortices. In this region Z_2 projection should fail to match the unprojected potential, and in fact that is what we see in Fig. 9, where the projected and unprojected potentials are compared at $\beta = 2.5,\ \gamma = 1.4$. The unprojected potential fits (24) with $\sigma \approx 0$, as already noted. Not so for the projected potential, where we find $\sigma = 0.00322(5)$. Moreover, the average plaquette value in this case is 0.887, while the average value of plaquettes whose location coincides with vortices on the projected lattice is 0.803. While there is

[5] The fact that plaquettes on the unprojected lattice, at vortex locations on the projected lattice, are not closer to -1 can be attributed to either a thickness of the vortex which is greater than one lattice spacing, and/or a small error, on the projected lattice, in finding the actual vortex location.

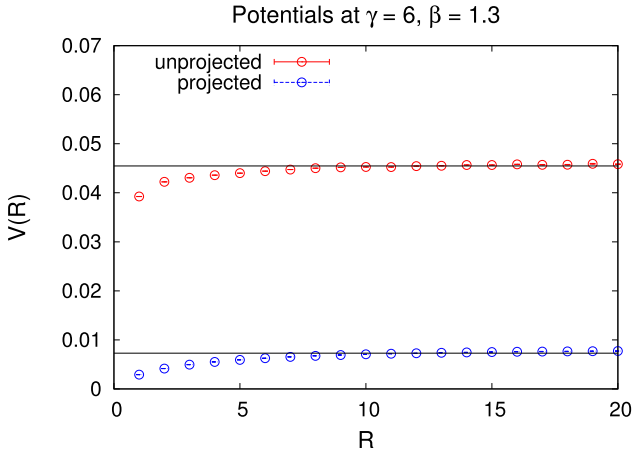

Fig. 7. The projected and unprojected potentials at a point inside the SC phase.

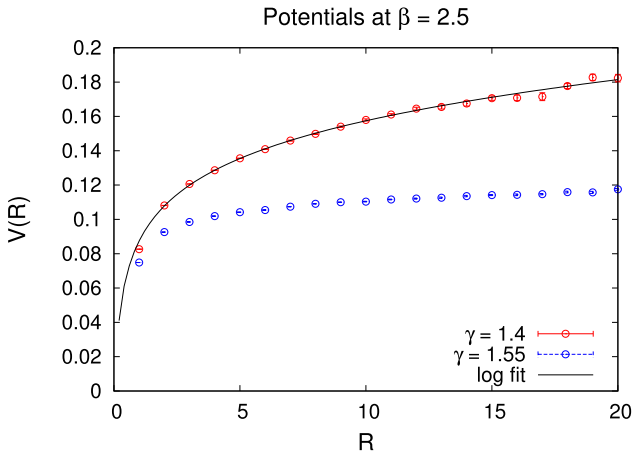

Fig. 8. The potential $V(R)$ at $\beta = 2.5$ just below ($\gamma = 1.4$) and just above ($\gamma = 1.55$) the superconducting transition line.

some modest correlation here between vortex location on the projected lattice and plaquette value on the unprojected lattice, it is greatly reduced as compared (0.909 vs. 0.398) to the previous case at $\beta = 1.1, \gamma = 6$, in a region described as a vortex liquid.

So the normal phase appears to have regions with and without a string tension, associated with the presence or absence, respectively, of vortex effects. We have been unable, however, to detect a thermodynamic phase transition between the vortex liquid and logarithmic potential regions, and it is numerically somewhat challenging to pin down exactly where the string tension disappears. To search for a thermodynamic transition from the behavior of the plaquette susceptibility we have scanned the phase diagram at fixed $\beta = 1.1$ and $0 < \gamma < 6$, and also at fixed $\gamma = 1.4$ and $0 < \beta < 2.5$. We have not found any evidence of a transition along these search lines, which cross from the vortex liquid to the log potential regions. The absence of a thermodynamic phase transition is perhaps unsurprising, since there is no symmetry which distinguishes the vortex liquid from the log potential regions. Indeed the vortex liquid and log potential regions are both "confining" in the sense that $V(R) \to \infty$ as $R \to \infty$ in each case, and consequently $\langle P \rangle = 0$ in both regions.

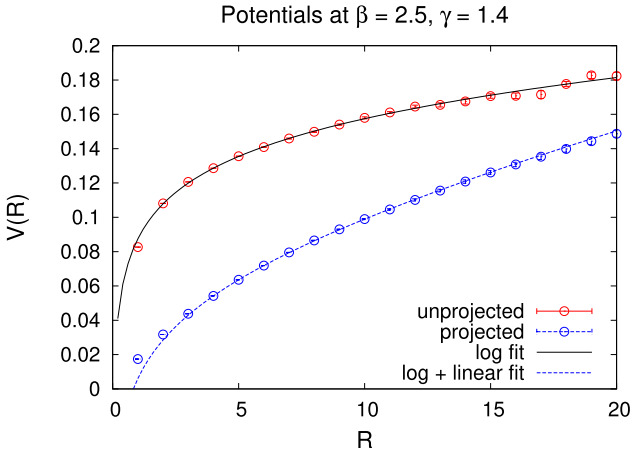

Fig. 9. A comparison of the projected and unprojected potentials in the normal phase, at $\beta = 2.5,\ \gamma = 1.4$. In this case the Z_2 projection is misleading.

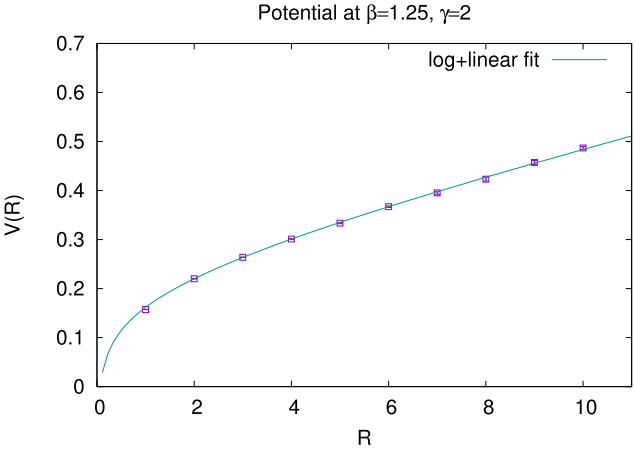

Fig. 10. The potential at $\beta = 1.25, \gamma = 2.0$ on a 40^3 lattice volume, computed at $R \leq 10$.

If it were possible to compute $V(R)$ out to $R = 20$ or larger everywhere in the phase diagram, then it might be possible to pinpoint the disappearance of the linear potential, but this strategy is frustrated, at small β, γ, by very large error bars on relatively small Wilson loops. As γ is reduced at small β, large Wilson loops become noisy, and we are not able to measure $V(R)$ up to the limit set by the lattice size. As an example, we show in Fig. 10 our results at $\beta = 1.25,\ \gamma = 2$, together with a best fit to (24). In this case we still find evidence of a linear potential with $\sigma = 0.0226(6)$; a purely logarithmic fit fails completely. However, at these couplings we cannot reliably go beyond $R = 10$ on the 40^3 lattice volume. Moreover, as γ is reduced the Z_2 projection becomes increasingly inaccurate, e.g. at $\beta = 1.25,\ \gamma = 2$ the Z_2 projected string tension is about 30% larger than the string tension derived from the unprojected data. As we increase β at fixed $\gamma = 1.4$ it is possible to again measure the potential at larger values of R, but the string tension seems to either gradually disappear, or else exists at R values beyond the practical limitations imposed by statistics and lattice size. In any case we cannot detect any trace of a linear potential at $\beta = 2.5,\ \gamma = 1.4$, as seen in Fig. 9.

The precise manner in which the disordering effects of the vortex liquid disappear in the normal phase as γ is reduced and β increased, whether that disappearance is sudden or gradual, and whether it is associated with some instability in the vortex configurations at small γ, is unclear at the moment. In the next section we will suggest that the transition from the logarithmic region to the linear potential region may be related to a spin glass transition.

5. A spin glass phase?

Although Elitzur's theorem rules out the breaking of a local gauge symmetry, it is always possible to impose a gauge condition, such as Coulomb or Landau or a maximal axial gauge, which preserves a global subgroup of the gauge group. Spontaneous breaking of such remnant symmetries is not forbidden by the Elitzur theorem, and some texts do define spontaneously broken gauge symmetry in this way, e.g. [25].[6] There are at least two problems with that idea, however. The first is that transition lines for remnant symmetry breaking may differ in different gauges [13]. The second is that in the cuprates, the Mermin–Wagner theorem forbids spontaneous breaking of any continuous symmetry, yet cuprates have a superconducting phase, which therefore defies characterization in terms of the breaking of a continuous symmetry.

Leaving aside the second issue for a moment, some authors have introduced gauge invariant order parameters for spontaneously broken gauge symmetry. It is not hard to construct such order parameters, but all of the ones we are aware of are based, either explicitly or implicitly, on a gauge choice. Let $g(x;U)$ be a gauge transformation to a gauge G such as Landau or Coulomb or maximal axial gauge, and we consider the order parameter

$$Q_x = g(x;U)\phi(x) \tag{31}$$

where $\phi(x)$ is the Higgs field. By construction, Q_x is invariant under local gauge transformations of U_μ and ϕ, but does transform under the remnant global gauge symmetry. Constructions of that type are found in the literature, e.g. in [27,28], where G is (implicitly) an axial gauge, or in [29], where G is lattice Landau gauge, or the Dirac order parameter (see, e.g., [30]) where G is Coulomb gauge. Although these order parameters are described as (and in fact are) locally gauge-invariant, it should be understood that a certain gauge choice, and therefore a certain arbitrariness, underlies these constructions. Evaluation of such Q observables, in the absence of gauge fixing, is completely equivalent to evaluating the expectation value $\langle\phi\rangle$ in a particular gauge, and the case $\langle\phi\rangle \neq 0$ means that the remnant global symmetry has been broken in that gauge.

In [16] we have proposed a different identification of the Higgs phase of a gauge-Higgs theory: the Higgs phase is the phase of a spontaneously broken custodial symmetry. The term "custodial symmetry" is adopted from the electroweak theory of particle physics, and refers to a global symmetry of the Higgs field which does not transform the gauge field. Let us first consider the lattice abelian Higgs action S_{GL} of (1), where $S_{GL} = S_W(U) + S_m(U,\phi)$ is the sum of a pure gauge Wilson action $S_W(U)$ and the part of the action involving the matter field $S_m(U,\phi)$. In this theory the custodial symmetry is the group of global U(1) transformations $\phi(x) \to e^{i\alpha}\phi(x)$. Because the Higgs field transforms also under local gauge transformations, its expectation value vanishes in the absence of gauge fixing, so the question is how to observe the breaking of custodial symmetry without fixing the gauge in some way. The proposal in [16] was made in the context of a non-abelian gauge Higgs theory, but applies equally to the abelian theory under consideration. The idea is to write the usual partition function as a sum of the partition functions of a spin system in an external gauge field, i.e.

$$Z = \int DU\ Z_{spin}[U] e^{-S_W(U)}\ , \tag{32}$$

where

$$Z_{spin}[U] = \int D\phi\ e^{-S_m(U,\phi)} \tag{33}$$

[6] In this connection, see also [26].

Since the gauge field is held constant in $Z_{spin}[U]$, the only symmetry of the "spin system" is the group of global transformations $\phi(x) \to e^{i\alpha}\phi(x)$, and this symmetry *can* break spontaneously, depending on the background gauge field, and the value of γ. For an operator $\Omega(\phi, U)$ we define the expectation value in the spin system

$$\overline{\Omega}(U) = \frac{1}{Z_{spin}(U)} \int D\phi \ \Omega(\phi, U) e^{-S_m(U,\phi)} \ , \tag{34}$$

Then the full expectation value is

$$\begin{aligned} \langle \Omega \rangle &= \frac{1}{Z} \int DUD\phi \ \Omega(\phi, U) e^{-S_{GL}} \\ &= \int DU \ \overline{\Omega}(U) P(U) \end{aligned} \tag{35}$$

where the spin system average $\overline{\Omega}(U)$ is evaluated in a background with U chosen from the probability distribution

$$P(U) = \frac{1}{Z} Z_{spin}[U] e^{-S_W(U)} \ . \tag{36}$$

If Ω is simply the scalar field $\phi(x)$ we may define

$$\overline{\phi}(x; U) = \frac{1}{Z_{spin}(U)} \int D\phi \ \phi(x; U) e^{-S_m} \ , \tag{37}$$

Because $U_i(x) = \exp[i\theta_i(x)]$ is not gauge fixed, and $\theta_i(x)$ will in general vary wildly with position, the same will be true of $\overline{\phi}(x; U)$, and we must expect the spatial average of this quantity to vanish, even if custodial symmetry in $Z_{spin}(U)$ is spontaneously broken. The proposal is instead to take the spatial average of a gauge-invariant and positive definite quantity

$$\begin{aligned} \Phi &= \frac{1}{V} \sum_{x,t} \langle |\overline{\phi}(x; U)| \rangle \\ &= \frac{1}{V} \sum_{x,t} \int DU |\overline{\phi}(x; U)| P(U) \\ &= \frac{1}{Z} \int DU \frac{1}{V} \sum_{x,t} e^{-S_W(U)} \left| \int D\phi \ \phi(x) e^{-S_m(U,\phi)} \right| \end{aligned} \tag{38}$$

Custodial symmetry is said to be spontaneously broken if $\Phi > 0$ in the $V \to \infty$ limit, but this does not imply long range correlations in any gauge-invariant observable [16]. It should be emphasized that there is no appeal whatever, in this formulation, to any choice of gauge.

The order parameter Φ is very closely related to the Edwards–Anderson [31] order parameter for spin glasses. Their original model, for Ising spins $S_x = \pm 1$ and in the absence of an external magnetic field, was

$$H_{EA} = -\sum_{\langle xy \rangle} J_{xy} S_x S_y \tag{39}$$

where J_{xy} is a set of random couplings taken from some probability distribution $P(J)$. Since the couplings are random, the spatial average of spins will tend to average to zero, so the order parameter is taken to be

$$\begin{aligned} \kappa &= \int \prod_{\langle ij \rangle} dJ_{ij} \left(\frac{1}{V} \sum_k (\overline{S}_k)^2 \right) P(J) \\ \overline{S}_i &= \frac{\prod_n \sum_{S_n} S_i e^{-H_{EA}}}{\prod_n \sum_{S_n} e^{-H_{EA}}} \end{aligned} \tag{40}$$

The analogy between Φ and κ is obvious. Instead of spins S_i we have a unimodular complex field $\phi(x)$, with squared link variables $U_j^2(x) = e^{2i\theta_j(x)}$ in S_m which play the role of the random couplings J_{ij}, and these link variables are drawn from the probability distribution $P(U)$ in (36), rather than the simpler (usually Gaussian) distributions assigned for $P(J)$. The symmetry of the Edwards–Anderson model is global Z_2, while in our case it is global U(1). And while Edwards–Anderson order parameter κ involves the square $(\overline{S}_i)^2$ of the spin average, our order parameter Φ involves the modulus $|\overline{\phi}(x;U)|$. But the general idea is the same.

In [16] we have argued, in the context of the SU(2) gauge-Higgs model with the Higgs field in the fundamental representation of the gauge group, that the Higgs and confinement regions are separated by the spontaneous breaking of a custodial symmetry, and also that the Higgs and confinement regions are distinguished physically by different realizations of confinement, which we have termed color (C) confinement in the Higgs region, and separation of charge (S_c) confinement in the confinement region. Our conjecture is that the custodial symmetry breaking transition, and the S_c-to-C confinement transition, coincide. In the abelian model S_{MGL} there is also somewhere a transition between logarithmic and linear confinement. Could it be that this transition is also associated with spontaneous breaking of a custodial symmetry, which we now identify as a spin glass transition?

At this point we must confront the Mermin–Wagner theorem, mentioned at the beginning of this section. The modified Ginzburg–Landau action S_{MGL} differs from S_{GL} in that the Higgs part of the action is a set of uncoupled actions in different xy-planes. As a result, the custodial symmetries $\phi(x) \to e^{i\alpha(z)}\phi(x)$ can be regarded as a $U(1) \times U(1) \times \cdots \times U(1)$ symmetry, where each $U(1)$ factor is an independent global symmetry acting in a particular xy plane at fixed z and which could, in principle, break spontaneously. The Φ order parameter could detect such symmetry breaking in $Z_{spin}(U)$, if it exists. But a true symmetry breaking transition of this kind would imply the breaking of a continuous $U(1)$ symmetry in two dimensions, and this is ruled out by the Mermin–Wagner theorem.

Despite this fact, we may note that in real materials that are thought to be spin glasses, it is even now not known whether the spin glass transition is a true thermodynamic transition, and whether the global symmetries are truly broken spontaneously in the spin glass phase [32]. Spin glasses are, however, characterized by metastable states with extremely long relaxation times, and this is a property which we can investigate numerically, even granting the fact that a true custodial symmetry breaking transition cannot exist in the system described by S_{MGL}. Keeping the background gauge field fixed, metastability can be observed in the time variable of a molecular dynamics simulation, or the time variable of Langevin evolution, or, as the most convenient choice, in terms of the number of lattice sweeps n_s, in a Monte Carlo simulation in which the scalar field is updated but the gauge field U is fixed. In this last case metastability implies very long autocorrelation times.

Our procedure, after initial thermalization, is to compute Φ via a "Monte-Carlo-within-a-Monte Carlo" simulation. This means that we update the scalar and gauge fields together, according to the usual Metropolis algorithm, for some number of sweeps (we chose one hundred). This generates a starting configuration, with the gauge field U chosen from the probability distribution (36). The data-taking sweep actually consists of n_s sweeps, in which the scalar field $\phi(x)$ is updated, but the gauge field $U_i(x)$ is held fixed. At each data-taking sweep we compute the average

$$|\overline{\phi}| = \frac{1}{V}\sum_x \frac{1}{n_s}\left|\sum_{n=1}^{n_s}\phi(x,n)\right| \tag{41}$$

where index n denotes the nth Monte Carlo sweep with U fixed. Then averaging $|\overline{\phi}|$ over all data-taking sweeps in the simulation gives us an estimate for $\Phi(n_s)$. If there were a true transition, then on general statistical grounds we would expect

$$\Phi(n_s) = \Phi_\infty + \frac{c}{\sqrt{n_s}} \tag{42}$$

with c a constant, and Φ_∞ non-zero in the case of a true transition. Because of the Mermin–Wagner theorem it must be that $\Phi(n_s) \to 0$ as $n_s \to \infty$, even in the infinite volume limit. But if there exist

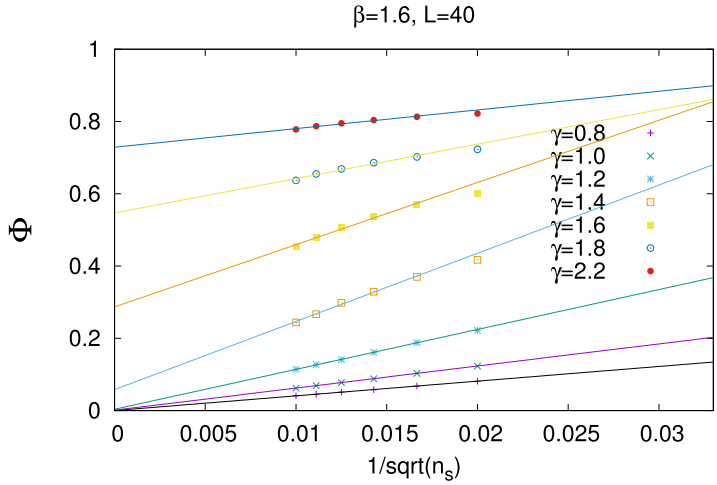

Fig. 11. The custodial symmetry/spin glass order parameter Φ vs. $1/\sqrt{n_s}$, where n_s is the number of update sweeps of the scalar field with the gauge field held fixed. The data shown is at $\beta = 1.6$ and γ values from 0.8 to 2.2 on a 40^3 lattice volume. The straight lines are best fits to the data at fixed β, γ. There is an (apparent) transition at a critical coupling γ_c between $\gamma = 1.2$ and 1.4, beyond which the extrapolated value of Φ at $n_s = \infty$ appears to be non-zero.

metastable states with very long relaxation times, it could be that, beyond some line of critical couplings, the large volume data fits (42) with $\Phi_\infty > 0$ up to very large values of n_s. This would indicate the existence of a line of quasi-transitions into a spin glass state of some kind, which is a precursor to genuine transitions in higher spatial dimensions.

In Fig. 11 we display our results for $\Phi(n_s)$ vs. $1/\sqrt{n_s}$, at $\beta = 1.6$, and various γ, computed on a 40^3 lattice volume. Data points in the figure were computed at n_s up to $n_s = 10000$. For γ below the quasi-transition point at $1.2 < \gamma_c < 1.4$, the data falls on a straight line which extrapolates to $\Phi_\infty = 0$ at $n_s \to \infty$. Above the transition, the data appears to extrapolate to a non-zero value of Φ_∞. By estimating at which γ value, for fixed β, the extrapolated value for Φ_∞ begins to move away from zero, we arrive at the quasi-transition points shown in Fig. 12.

Of course, at $n_s \to \infty$ we must have $\Phi_\infty \to 0$, in a finite volume, even if there were a true transition in the infinite volume limit. In Fig. 13 we show the data at $\beta = 0.8, \gamma = 2.2$, which is inside the linearly confining region which have argued corresponds to the pseudogap region in cuprates, on $20^3, 40^3, 80^3$ lattice volumes, up to $n_s = 20{,}000$ lattice sweeps. At all three volumes we see the data fall away from the straight line (a fit to the first few data points at low n_s), presumably heading to zero at $n_s = \infty$. The falloff is, however, most pronounced at the smallest 20^3 volumes, and the data points seem to tend upwards towards the straight line as the volume increases. Were it not for the Mermin–Wagner theorem, we would probably conclude that Φ_∞ is non-zero in the infinite volume limit. This cannot be true. Nevertheless, there is no strong indication from the data that Φ_∞ vanishes at infinite volumes, and this implies the existence of states with very long relaxation times as measured by the n_{spin}, parameter, characteristic of some sort of spin glass phase, with a fairly abrupt transition, as γ varies at fixed β, to a phase of this kind. We regard this as a precursor to the true custodial symmetry breaking transition expected in higher dimensions. Our conjecture is that this quasi-transition is associated with a transition from the massless phase, i.e. logarithmic confinement, to the "gapped" phases, namely the pseudogap and superconducting phases.

6. Towards a realistic effective action

In this article we have advocated the use of electromagnetic observables, i.e. Wilson loops, Polyakov loops, and Z_2 projected Wilson loops, as a probe of cuprate phase structure, and in

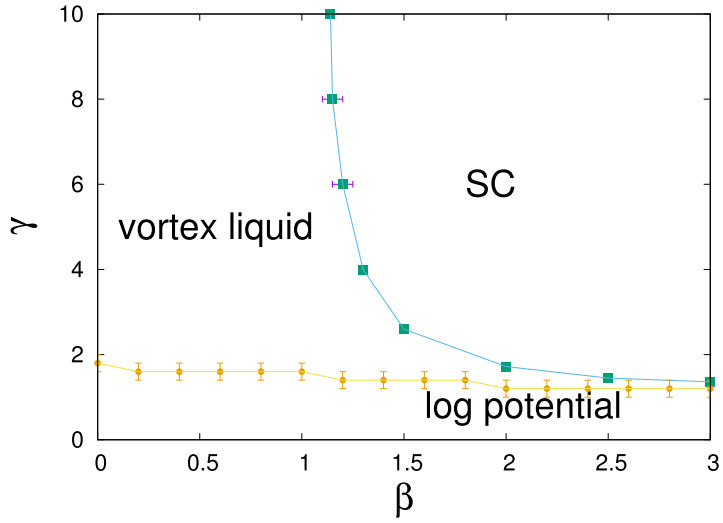

Fig. 12. Location of the spin glass "quasi-transition" (yellow circles) in the phase diagram of the modified Ginzburg–Landau lattice action.

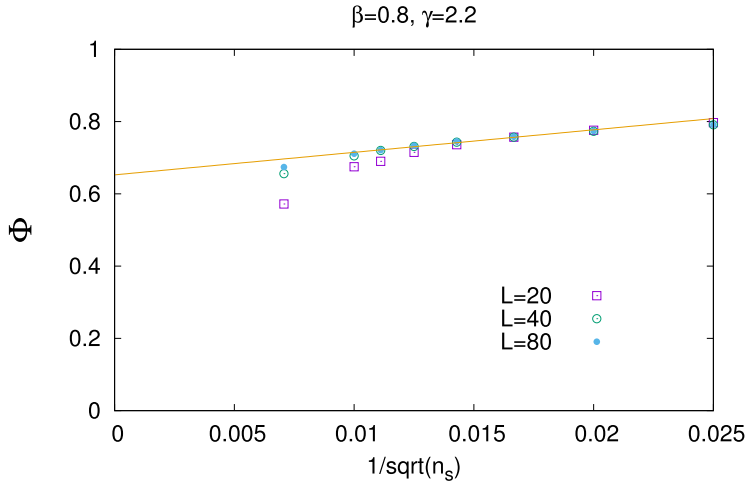

Fig. 13. The spin glass order parameter $\Phi(n_s)$ vs. $1/\sqrt{n_s}$ at $\beta = 0.8, \gamma = 2.2$, computed on lattice volumes L^3 with $L = 20, 40, 80$. In this case the simulations were carried out to $n_s = 20{,}000$.

particular we have argued that there are strong analogies between the pseudogap phase of the cuprates, and the confined phase of a non-abelian gauge theory. However, we have illustrated the use of those observables in a theory which, while incorporating certain important features, is surely not a very realistic model of the cuprates. For one thing, the momentum-space anisotropies associated with D-wave superconductivity are absent in this model, and so it goes wrong already at this early stage. In addition, if we take e.g. $T = 100$ K and β to be of O(1) we get a lattice spacing on the order of 10^{-4} m (see footnote 1), and this is far larger than the radius of a magnetic vortex in a cuprate, which is the scale where we might expect the effective theory to apply. In this section we would like to indicate how one might derive, and solve numerically, a more realistic model.

The obvious starting point is the Hubbard model Hamiltonian

$$\begin{aligned} H &= -\mathbf{q}\sum_x\sum_{i=1}^{2}\Big(c^\dagger_\sigma(x)c_\sigma(x+\hat{\imath})+c^\dagger_\sigma(x)c_\sigma(x-\hat{\imath})\Big) \\ &\quad +\mathbf{Y}\sum_x(n_\uparrow(x)-\frac{1}{2})(n_\downarrow(x)-\frac{1}{2})-\overline{\boldsymbol{\mu}}\sum_x(n_\uparrow(x)+n_\downarrow(x)) \\ &= H_K+H_V \end{aligned} \tag{43}$$

where H_K is the hopping term proportional to $\mathbf{q}$, H_V contains the local terms proportional to $\mathbf{Y}$, $\overline{\boldsymbol{\mu}}$, and constants $\mathbf{q}, \mathbf{Y}, \overline{\boldsymbol{\mu}}$ all have units of energy, and

$$Z(\beta) = \mathrm{Tr}\; e^{-\beta H} \tag{44}$$

We have made the slight generalization that the sum over x in (43) is taken to be a sum over sites in a *three*-dimensional lattice. Electrons hop only between nearest sites in planes parallel to the x–y plane, so at this initial stage the introduction of numerous planes perpendicular to the z-axis is just a redundancy.

Lattice Monte Carlo treatments of the Hubbard model are generally based on the seminal work of Blankenbecler, Scalapino, and Sugar (BSS) [33] (see e.g. the early studies in [34,35], and more recent investigations in [36–41]), and we will also follow along these lines. In order to address the questions we are interested in we have to modify the model to include the electromagnetic field, and also explain how we would deal with the sign problem, which is inevitable away from half-filling. The electromagnetic field is introduced in a fairly obvious way, by following along the BSS derivation and then imposing local gauge invariance. We suggest here that the sign problem might be addressed by the complex Langevin approach. We should stress that this section does not contain any numerical results; it is only a proposal. The calculation that we outline here is computationally intensive, and is reserved for future work.

Starting from

$$Z = \mathrm{Tr}\; e^{-\beta H} = \mathrm{Tr}\left(e^{-\delta t H}\right)^{N_t} \approx \mathrm{Tr}\left(e^{-\delta t H_K}e^{-\delta t H_V}\right)^{N_t} \tag{45}$$

where $\delta t = \beta/N_t$, we define the dimensionless constants

$$q = \beta\mathbf{q}\;\;,\;\;\; Y = \beta\mathbf{Y}\;\;,\;\;\; \mu = \beta\overline{\boldsymbol{\mu}} \tag{46}$$

Then re-express the term proportional to Y via the Hubbard–Stratonovich transformation

$$\begin{aligned} \exp\left[-\frac{1}{N_t}Y(n_\uparrow(x)-\frac{1}{2})(n_\downarrow(x)-\frac{1}{2})\right] &= \left(\frac{1}{N_t\pi}\right)^{\frac{1}{2}}e^{-Y/4N_t} \\ &\quad\times\int d\phi(x)\exp\left[-\frac{1}{N_t}(\phi^2(x))+\sqrt{2Y}(n_\uparrow(x)-n_\downarrow(x))\right] \end{aligned} \tag{47}$$

It was shown by BSS that the partition function (45) can be rewritten as a Euclidean time path integral over bosonic (ϕ) and Grassman ($\overline{\psi}, \psi$) valued fields

$$Z = \int\prod_{t=1}^{N_t}\prod_x d\overline{\psi}_\sigma(x,t)d\psi_\sigma(x,t)d\phi(x,t)\; e^{-S} \tag{48}$$

where

$$S = \frac{1}{N_t}\sum_{x,t}\phi^2(x,t)+\sum_{x,x'}\sum_{t,t'}\sum_{\sigma=\uparrow,\downarrow}\overline{\psi}_\sigma(x,t)M_\sigma(xt,x't')\psi_\sigma(x',t') \tag{49}$$

with

$$M_\sigma = \begin{bmatrix} \mathbb{1} & 0 & 0 & \cdots & B_1^\sigma \\ -B_2^\sigma & \mathbb{1} & 0 & \cdots & 0 \\ 0 & -B_3^\sigma & \mathbb{1} & \cdots & 0 \\ \cdot & \cdot & \cdot & & 0 \\ \cdot & \cdot & \cdot & & 0 \\ \cdot & \cdot & \cdot & & 0 \\ \cdot & \cdot & \cdots & -B_{N_t}^\sigma & \mathbb{1} \end{bmatrix} \tag{50}$$

In this expression the time index t' runs left to right, index t runs along the vertical, $\mathbb{1}$ and B_t^σ are matrices of dimension $N_S \times N_S$, where N_S is the total number of lattice sites, and where

$$B_t^\sigma = e^{-K/N_t} e^{-V_s/N_t} \tag{51}$$

with

$$K(x,y) = -q \sum_{i=1,2} (\delta_{x+\hat{\imath},y} + \delta_{x-\hat{\imath},y})$$

$$V_\sigma(x,y) = \delta_{xy}(\mu + s_\sigma \sqrt{2Y}\phi(x,t)) \quad \text{where} \quad s_\sigma = \begin{cases} +1 & \sigma = \uparrow \\ -1 & \sigma = \downarrow \end{cases} \tag{52}$$

Integrating over the Grassman variables leads to an effective action for the Hubbard–Stratonovich field

$$\begin{aligned} Z &= \int \prod_{t=1}^{N_t} \prod_x d\phi(x,t) \det[M_\uparrow] \det[M_\downarrow] \exp\left[-\frac{1}{N_t} \sum_{t=1}^{N_t} \sum_x \phi^2(x,t) \right] \\ &= \int \prod_{t=1}^{N_t} \prod_x d\phi(x,t) e^{-S_\phi} \end{aligned} \tag{53}$$

where

$$S_\phi = \frac{1}{N_t} \sum_{t=1}^{N_t} \sum_x \phi^2(x,t) - \mathrm{Tr} \ln M_\uparrow - \mathrm{Tr} \ln M_\downarrow \tag{54}$$

In the case of half filling it can be shown that $\det[M_\uparrow]$ and $\det[M_\downarrow]$ have the same sign [34], so there is no sign problem in that situation. So far this is all standard.

The next step is to promote the global invariance of (49) under $\underline{\psi} \to e^{i\alpha}\psi$, $\overline{\psi} \to e^{-i\alpha}\overline{\psi}$ to a local invariance, keeping in mind that the $N_S \times N_S$ matrix B_t connects $\overline{\psi}$ at time t with ψ at time $t-1$. Local invariance is achieved by first modifying the hopping term

$$K(x,y) \to K_U(x,y) = -q \sum_{i=1,2} (\delta_{x+\hat{\imath},y} U_i(x,t) + \delta_{x-\hat{\imath},y} U_i^\dagger(x-\hat{\imath})) \tag{55}$$

and then, since M_σ connects ψ at time $t-1$ to $\overline{\psi}$ at time t, we introduce the diagonal matrix $\mathcal{U}_t$ with matrix elements

$$[\mathcal{U}_t]_{xy} = \delta_{xy} U_4^\dagger(x, t-1) \tag{56}$$

and redefine

$$B_t^\sigma = \mathcal{U}_t e^{-K_U/N_t} e^{-V_\sigma/N_t} \tag{57}$$

We then add the latticized action S_W for the electromagnetic field to the effective action. Here we must take account of the different lattice spacings that are involved. The Hubbard model assumes that electrons hop in a plane, between points separated by some spacing a. The neighboring planes are separated by a distance a_z, with a and a_z at the interatomic distance scale, presumed to be fixed (like $\mathbf{q}, \mathbf{Y}$) by comparison to some real material. The Euclidean time step is $\delta t = \beta/N_t$, with continuous time obtained in the $N_t \to \infty$ limit. With gauge link variables $U_\mu(x) = \exp[i\theta_\mu(x)]$

and $\theta_{\mu\nu}$ defined in (2), the Wilson lattice action for this asymmetric lattice, having the appropriate continuum limit, is

$$S_W = -\frac{1}{e^2}\sum_x \left\{ \frac{N_t}{\beta}\left(a_z(\cos\theta_{14}+\cos\theta_{24}) + \frac{a^2}{a_z}\cos\theta_{34}\right) + \frac{\beta}{N_t}\left(\frac{1}{a_z}(\cos\theta_{13}+\cos\theta_{23}) + \frac{a_z}{a^2}\cos\theta_{12}\right)\right\} \tag{58}$$

The final effective action is

$$S_{eff}(\theta_\mu,\phi) = S_\phi(\theta_\mu,\phi) + S_W(\theta_\mu) \tag{59}$$

where S_ϕ is the action in (54) with the modification (57). For arbitrary chemical potential there is certainly a sign problem.

We are not aware of any numerical treatment of the Hubbard model which incorporates a coupling to the quantized electromagnetic field, probably because this field is considered extraneous to the underlying physics. The experimental evidence of vortex effects in the pseudogap phase of cuprates suggests that this coupling should not be ignored. However, with or without the coupling to the electromagnetic field, one must confront the sign problem in regions of interest in the cuprate phase diagram. There are a number of approaches in the literature. One idea, which goes back to [35], is to simulate the theory using the modulus $|\det M_\uparrow \det M_\downarrow|$. This is known as the "sign-quenched" technique in the particle physics literature, and it is known to go wrong for QCD at high baryon density [42]. Three other methods which have been studied extensively are the complex Langevin equation [43–45], the thimble approach [46], and the LLR algorithm [47]. None of these methods is perfect. Each has been shown to work successfully in some models, and to fail in others. The thimble approach has recently been applied to the two-dimensional Hubbard model [40,41], but thus far only for tiny (2×2) lattices.

We propose to apply the complex Langevin equation to the effective Hubbard model action which includes the quantized gauge field. Discretizing the fictitious Langevin time τ, the Langevin equations are

$$\begin{aligned}\phi(x,t,\tau+\epsilon) &= -\left[\frac{\partial S_{eff}}{\partial\phi(x,t)}\right]_\tau \epsilon + \eta_\phi(x,t,\tau)\sqrt{\epsilon}\\ \theta_\mu(x,t,\tau+\epsilon) &= -\left[\frac{\partial S_{eff}}{\partial\theta_\mu(x,t)}\right]_\tau \epsilon + \eta_{\theta_\mu}(x,t,\tau)\sqrt{\epsilon}\end{aligned} \tag{60}$$

where the notation $[...]_\tau$ means that the quantity in brackets is to be evaluated with fields at Langevin time τ, and the η fields are random numbers with a probability distribution such that

$$\begin{aligned}\langle\eta_\phi(x,t,\tau)\eta_\phi(x',t',\tau')\rangle &= 2\delta_{xx'}\delta_{tt'}\delta_{\tau\tau'}\\ \langle\eta_{\theta_\mu}(x,t,\tau)\eta_{\theta_\nu}(x',t',\tau')\rangle &= 2\delta_{\mu\nu}\delta_{xx'}\delta_{tt'}\delta_{\tau\tau'}\\ \langle\eta_\phi(x,t,\tau)\eta_{\theta_\mu}(x',t',\tau')\rangle &= 0\end{aligned} \tag{61}$$

Since the effective action S_{eff} is in general complex away from half-filling, these equations are only consistent if the ϕ,θ_μ fields are also complex (and of course this means that gauge link variables are no longer unimodular), but the η fields are always taken to be real. Solving these equations numerically, and averaging observables over the fictitious Langevin time, is the essence of the complex Langevin approach.

The trace of logarithms in the effective action give rise to

$$\begin{aligned}-\frac{\partial S_{eff}}{\partial\phi(x,t)} &= -\frac{2}{N_t}\phi(x,t) + \sum_{\sigma=\uparrow,\downarrow}\mathrm{Tr}\left[M_\sigma^{-1}\frac{\partial}{\partial\phi(x,t)}M_\sigma\right]\\ -\frac{\partial S_{eff}}{\partial\theta_\mu(x,t)} &= -\frac{\partial S_W}{\partial\theta_\mu(x,t)} + \sum_{\sigma=\uparrow,\downarrow}\mathrm{Tr}\left[M_\sigma^{-1}\frac{\partial}{\partial\theta_\mu(x,t)}M_\sigma\right]\end{aligned} \tag{62}$$

Since M_σ has dimensions of $N \times N$, where $N = N_t N_S$ is the number of lattice sites, direct inversion of M_σ at each Langevin time step is impractical if N is large, but there are tricks which avoid direct inversion, as explained in, e.g., [44]. The idea is to approximate the trace with a stochastic N-component noise vector $\mathbf{v}$

$$\mathrm{Tr}\left[M_\sigma^{-1}\partial M_\sigma\right] \approx \mathbf{v}^\dagger \cdot M_\sigma^{-1}\partial M_\sigma \mathbf{v} \tag{63}$$

where $\mathbf{v}$ is drawn from a Gaussian probability distribution such that

$$\langle v_i^* v_j\rangle = \delta_{ij} \tag{64}$$

One must then solve the linear system

$$M_\sigma^\dagger \mathbf{w} = \mathbf{v} \tag{65}$$

after which the trace becomes

$$\mathrm{Tr}\left[M_\sigma^{-1}\partial M_\sigma\right] \approx \mathbf{w}^\dagger \cdot \partial M_\sigma \mathbf{v} \tag{66}$$

The most computationally intensive part of this algorithm is the solution of the linear system of equations (65). This is practical if the matrix M_σ is sparse, which is not quite true of the $N_S \times N_S$ matrix B_t^σ. The problem is that while the matrix K_U is sparse, the exponential of this matrix is not. One possibility is to expand $\exp[-K_U/N_t]$ to first or second order in $1/N_t$, in which case M_σ will be a sparse matrix. There are indications that expansion to first order may not be sufficient, cf. [38] unless N_t is quite large, and this reference also presents a method (the "Schur complement solver"), which speeds up the solution of the linear system without approximating the exponential $\exp[-K_U/N_t]$. The method has also been applied in the thimble approach of [40]. Alternatively, one might simply expand $\exp[-K_U/N_t]$ to second order in $1/N_t$.

By these means it ought to be possible implement evolution in Langevin time and to compute gauge field observables, in particular Wilson loops, Polyakov loops, vortex densities, electromagnetic field strengths, and so on. The complex Langevin method is practical, and supplies numerical answers to numerical questions. What is not certain is whether those answers are correct. The validity of the method is not guaranteed when the action is non-holomorphic [48,49], which is the situation for the Hubbard model. Sometimes the complex Langevin approach will supply the correct answers for non-holomorphic actions, and sometimes not [50]. There are certain tests for validity; one can only try and see.

The effective action S_{eff} in (59), unlike our modified Ginzburg–Landau model (4), is not a gauge-Higgs theory in the usual sense because the scalar Hubbard–Stratonovich field is uncharged. If we are only interested in gauge field observables, this is not a problem. It has been suggested (in the context of graphene) that effective theories involving the charge-neutral Hubbard–Stratonovich field (but not the gauge field) can be used to detect charge and spin density wave order [38]. On the other hand, a theory with a neutral scalar field cannot be used to investigate the possible spin-glass nature of the Higgs and pseudogap phases, as suggested in the last section. So the question is whether one could follow the steps in the derivation of the Ginzburg–Landau theory from the BCS Hamiltonian, as presented in many textbooks (e.g. [51]), using a charged rather than a neutral Hubble–Stratonovich field to decouple the four-fermi interaction term. The problem, however, is that unlike the BCS Hamiltonian, where the four-fermi attraction is attractive, in the Hubbard model the four-fermi term is repulsive, and the opposite sign of this term as compared to the BCS theory results in a "wrong-sign" in front of the term $\phi^*(x)\phi(x)$ quadratic in the Hubbard–Stratonovich field, i.e. if one could argue that the integral

$$\int d\phi \exp[(\phi^* - \sqrt{Y}c_\uparrow^\dagger c_\downarrow^\dagger)(\phi - \sqrt{Y}c_\downarrow c_\uparrow)/N_t] \tag{67}$$

was meaningful, then the Hubbard–Stratonovich trick would replace the four-fermi term in the Hubbard model Hamiltonian by the identity

$$\begin{aligned} &-(\phi^* - \sqrt{Y}c_\uparrow^\dagger c_\downarrow^\dagger)(\phi - \sqrt{Y}c_\downarrow c_\uparrow) + Y c_\uparrow^\dagger(x)c_\uparrow(x)c_\downarrow^\dagger(x)c_\downarrow(x) \\ &\quad = -\phi^*(x)\phi(x) + \sqrt{Y}\phi^*(x)c_\downarrow(x)c_\uparrow(x) + \phi(x)\sqrt{Y}c_\uparrow^\dagger(x)c_\downarrow^\dagger(x) \end{aligned} \tag{68}$$

with the obvious drawback that the integration over ϕ in $e^{-\beta H}$ is exponentially divergent. The situation is not necessarily hopeless. Wrong-sign quadratic terms have been encountered elsewhere, notably in Euclidean quantum gravity, where the kinetic term of the metric conformal factor has the wrong sign, and the recommended prescription [52] is to interpret expectation values of this field via a deformation of the contour of integration in the path integral. According to this prescription one would have, e.g.

$$\langle x^2 \rangle = \frac{\int dx\ x^2 e^{+x^2}}{\int dx\ e^{+x^2}} = -\frac{1}{2} \tag{69}$$

Another approach to so-called "bottomless action" theories, where the value of the Euclidean action is unbounded from below, is presented in [53]. But of course the difficulties of the wrong-sign term, coupled with the already thorny technicalities of the sign problem associated with the chemical potential, suggests that attention should be directed first to the effective theory with a neutral Hubbard–Stratonovich term, and a conventional sign in front of the quadratic term in the effective action.

Perhaps the greatest advantage of focussing on electromagnetic observables, i.e. Wilson loops, Polyakov lines, and center-projected loops is that they allow us to study numerically the electromagnetic properties of the theory in the superconducting, pseudogap, and other phases of the theory even if the effective theory involves only a neutral Hubbard–Stratonovich field, which may be the only practical possibility.

7. Conclusions

We have presented a modified lattice version of the time-independent Ginzburg–Landau model, containing a compact U(1) gauge field with a no-monopole constraint, and an action for the scalar field with nearest-neighbor couplings limited to two dimensional x–y planes of the three dimensional volume. In this model we detect in numerical simulations

1. an area-law falloff for Wilson loops in the x–y planes, in regions of small β and large γ;
2. a superconducting phase at large β and large γ;
3. a falloff consistent with a logarithmic potential at large β and small γ.

The superconducting phase is distinguished from other regions of the phase diagram by the spontaneous breaking of a global Z_2 symmetry.

In the region of area-law falloff we have used a Z_2 projection procedure to identify the location of vortex configurations, and provided evidence that the identified vortices are responsible for the area-law falloff. This ties in to the center vortex theory of confinement in non-abelian gauge theories, as briefly reviewed here. It is interesting that this is an example where the introduction of a matter field can induce an area-law falloff in a U(1) gauge theory with a no-monopole constraint, in which the area-law falloff would otherwise be absent.

While we do not suggest that the modified lattice Ginzburg–Landau model studied here is a realistic model of the physics of cuprates, we do believe that it furnishes an example of a superconducting to vortex liquid phase in the context of a U(1) gauge theory, in which the modulus of the scalar field is a non-zero constant. This may be relevant to the superconducting to pseudogap transition found in the cuprates.

On the experimental side, we note that there have, in fact, been measurements of magnetic susceptibility along a planar area of a thin film of cuprate material in the superconducting phase, e.g. [54]. Perhaps it is also feasible to compute the expectation value of Wilson loops of fixed area in the pseudogap phase. This could be accomplished by measuring the magnetic flux $\Phi(t)$ through a fixed loop C as a function of time, from which we derive the corresponding Wilson loop observable $\exp[ie\Phi(t)/\hbar]$, also as a function of time, and then averaging with respect to time to determine $W(C)$. The behavior of Wilson loops is fundamental to our understanding of the strong nuclear force, so their experimental determination in cuprate materials is an intriguing possibility.

We finally wish to stress the utility of gauge field observables in the numerical simulation of more realistic theoretical models of the cuprates, such as the Hubbard model. This calls for

introducing the electromagnetic gauge field in such models, as discussed in the previous section. There is no need, in this approach, to have a charged order parameter associated with pairing, e.g. a charged Hubbard–Stratonovich field in the effective action. The distinction between the normal, superconducting, and pseudogap phases can be made entirely in terms of gauge field observables, i.e. the Wilson, Polyakov, and Z_2-projected loops, and the challenge is mainly to confront the sign problem, perhaps via the complex Langevin equation, or by some other means.

Declaration of competing interest

The authors declare that they have no known competing financial interests or personal relationships that could have appeared to influence the work reported in this paper.

Acknowledgments

We thank Makoto Hashimoto for discussions. JG's research is supported by the U.S. Department of Energy under Grant No. DE-SC0013682.

References

[1] Y. Wang, L. Li, N. Ong, Phys. Rev. B 73 (2) (2006) 024510, arXiv:cond-mat/0510470.
[2] L. Li, Y. Wang, M. Naughton, S. Komiya, S. Ono, Y. Ando, N. Ong, J. Magn. Magn. Mater. 310 (2007) 460–466, arXiv:cond-mat/0611731.
[3] L. Li, Y. Wang, S. Komiya, S. Ono, Y. Ando, G. Gu, N. Ong, Phys. Rev. B 81 (5) (2010) 054510, arXiv:0906.1823.
[4] P. Anderson, Four last conjectures, 2018, ArXiv e-prints, arXiv:1804.11186.
[5] P. Anderson, Last words on the cuprates, 2016, ArXiv e-prints, arXiv:1612.03919.
[6] V.J. Emery, S.A. Kivelson, Phys. Rev. Lett. 74 (1995) 3253–3256.
[7] S. Sachdev, H.D. Scammell, M.S. Scheurer, G. Tarnopolsky, Phys. Rev. B 99 (2019) 054516, http://dx.doi.org/10.1103/PhysRevB.99.054516.
[8] T.A. DeGrand, D. Toussaint, Phys. Rev. D22 (1980) 2478, 194 (1980).
[9] G. Mack, V.B. Petkova, Z. Phys. C12 (1982) 177.
[10] S. Elitzur, Phys. Rev. D12 (1975) 3978–3982.
[11] K. Osterwalder, E. Seiler, Ann. Physics 110 (1978) 440.
[12] E.H. Fradkin, S.H. Shenker, Phys. Rev. D19 (1979) 3682–3697.
[13] W. Caudy, J. Greensite, Phys. Rev. D78 (2008) 025018, arXiv:0712.0999.
[14] S. Willenbrock, Symmetries of the standard model, arXiv:hep-ph/0410370.
[15] A. Maas, Prog. Part. Nucl. Phys. 106 (2019) 132–209, http://dx.doi.org/10.1016/j.ppnp.2019.02.003.
[16] J. Greensite, K. Matsuyama, Phys. Rev. D98 (7) (2018) 074504, arXiv:1805.00985.
[17] G. 't Hooft, Nuclear Phys. B138 (1978) 1–25.
[18] J. Greensite, Springer Lect. Notes Phys. 821 (2011) 1–211.
[19] J. Greensite, Prog. Part. Nucl. Phys. 51 (2003) 1, arXiv:hep-lat/0301023.
[20] M. Engelhardt, K. Langfeld, H. Reinhardt, O. Tennert, Phys. Lett. B431 (1998) 141–146, arXiv:hep-lat/9801030.
[21] W. Kamleh, D. Leinweber, D. Trewartha, Proceedings, 26th International Nuclear Physics Conference (INPC2016): Adelaide, Australia, September 11–16, 2016, PoS INPC2016 (2017) 293.
[22] D. Trewartha, W. Kamleh, D. Leinweber, Centre vortex removal restores chiral symmetry, 2017, arXiv:1708.06789.
[23] J. Greensite, K. Matsuyama, Phys. Rev. D96 (9) (2017) 094510, http://dx.doi.org/10.1103/PhysRevD.96.094510, arXiv:1708.08979.
[24] A.M. Polyakov, Nuclear Phys. B120 (1977) 429–458.
[25] A. Duncan, The Conceptual Framework of Quantum Field Theory, in: EBSCO Ebook Academic Collection, OUP Oxford, 2012, https://books.google.com/books?id=MuH0TQvpY5sC.
[26] M. Greiter, Ann. Physics 319 (1) (2005) 217–249, http://dx.doi.org/10.1016/j.aop.2005.03.008.
[27] A.M. Schakel, Boulevard of broken symmetries, 1998, ArXiv preprint, cond-mat/9805152.
[28] J. van Wezel, J. van den Brink, Phys. Rev. B77 (6) (2008) 064523, http://dx.doi.org/10.1103/PhysRevB.77.064523, arXiv:0706.1922.
[29] T. Kennedy, C. King, Comm. Math. Phys. 104 (1986) 327–347, http://dx.doi.org/10.1007/BF01211599.
[30] T.H. Hansson, V. Oganesyan, S.L. Sondhi, Ann. Physics 313 (2) (2004) 497–538, http://dx.doi.org/10.1016/j.aop.2004.05.006.
[31] S.F. Edwards, P.W. Anderson, J. Phys. F 5 (5) (1975) 965–974.
[32] D.L. Stein, C.M. Newman, Complex Syst. 20 (2011).
[33] R. Blankenbecler, D.J. Scalapino, R.L. Sugar, Phys. Rev. D24 (1981) 2278.
[34] J.E. Hirsch, Phys. Rev. B31 (1985) 4403–4419.
[35] S.R. White, D.J. Scalapino, R.L. Sugar, E.Y. Loh, J.E. Gubernatis, R.T. Scalettar, Phys. Rev. B40 (1989) 506–516, http://dx.doi.org/10.1103/PhysRevB.40.506.

[36] D. Smith, L. von Smekal, Phys. Rev. B89 (19) (2014) 195429, http://dx.doi.org/10.1103/PhysRevB.89.195429, arXiv:1403.3620.
[37] S. Beyl, F. Goth, F.F. Assaad, Phys. Rev. B97 (8) (2018) 085144, http://dx.doi.org/10.1103/PhysRevB.97.085144, arXiv:1708.03661.
[38] P. Buividovich, D. Smith, M. Ulybyshev, L. von Smekal, Phys. Rev. B98 (23) (2018) 235129, http://dx.doi.org/10.1103/PhysRevB.98.235129, arXiv:1807.07025.
[39] E.W. Huang, R. Sheppard, B. Moritz, T.P. Devereaux, Strange metallicity in the doped Hubbard model, 2018, arXiv:1806.08346.
[40] M. Ulybyshev, C. Winterowd, S. Zafeiropoulos, Taming the sign problem of the finite density Hubbard model via Lefschetz thimbles, 2019, arXiv:1906.02726.
[41] M. Fukuma, N. Matsumoto, N. Umeda, Applying the tempered Lefschetz thimble method to the Hubbard model away from half-filling, 2019, arXiv:1906.04243.
[42] J.R. Ipsen, K. Splittorff, Phys. Rev. D86 (2012) 014508, http://dx.doi.org/10.1103/PhysRevD.86.014508, arXiv:1205.3093.
[43] G. Aarts, L. Bongiovanni, E. Seiler, D. Sexty, I.-O. Stamatescu, Eur. Phys. J. A49 (2013) 89, http://dx.doi.org/10.1140/epja/i2013-13089-4, arXiv:1303.6425.
[44] D. Sexty, Phys. Lett. B729 (2014) 108–111, http://dx.doi.org/10.1016/j.physletb.2014.01.019, arXiv:1307.7748.
[45] C.E. Berger, L. Rammelmüller, A.C. Loheac, F. Ehmann, J. Braun, J. n E. Drut, Complex langevin and other approaches to the sign problem in quantum many-body physics, 2019, arXiv:1907.10183.
[46] M. Cristoforetti, F. Di Renzo, A. Mukherjee, L. Scorzato, Phys. Rev. D88 (5) (2013) 051501, http://dx.doi.org/10.1103/PhysRevD.88.051501, arXiv:1303.7204.
[47] K. Langfeld, Proceedings, 34th International Symposium on Lattice Field Theory (Lattice 2016): Southampton, UK, July 24–30, 2016, PoS LATTICE2016 (2017) 010, http://dx.doi.org/10.22323/1.256.0010, arXiv:1610.09856.
[48] A. Mollgaard, K. Splittorff, Phys. Rev. D88 (2013) 116007, http://dx.doi.org/10.1103/PhysRevD.88.116007, arXiv:1309.4335.
[49] G. Aarts, E. Seiler, D. Sexty, I.-O. Stamatescu, J. High Energy Phys. 05 (2017) 044, J. High Energy Phys. 01 (2018) 128 (erratum), http://dx.doi.org/10.1007/JHEP05(2017)044, http://dx.doi.org/10.1007/JHEP01(2018)128, arXiv:1701.02322.
[50] J. Greensite, Phys. Rev. D90 (11) (2014) 114507, http://dx.doi.org/10.1103/PhysRevD.90.114507, arXiv:1406.4558.
[51] A. Altland, B.D. Simons, Condensed Matter Field Theory, second ed., Cambridge University Press, 2010, http://dx.doi.org/10.1017/CBO9780511789984.
[52] G.W. Gibbons, S.W. Hawking, M.J. Perry, Nuclear Phys. B138 (1978) 141–150, http://dx.doi.org/10.1016/0550-3213(78)90161-X.
[53] J. Greensite, M.B. Halpern, Nuclear Phys. B242 (1984) 167–188, http://dx.doi.org/10.1016/0550-3213(84)90138-X.
[54] S.I. Davis, R.R. Ullah, C. Adamo, C.A. Watson, J.R. Kirtley, M.R. Beasley, S.A. Kivelson, K.A. Moler, Phys. Rev. B 98 (2018) 014506.